Supporting Information for

Acid Strength and Bifunctional Catalytic Behavior of Alloys Comprised of Noble Metals and Oxophilic Metal Promoters

David Hibbitts, Qiaohua Tan, and Matthew Neurock

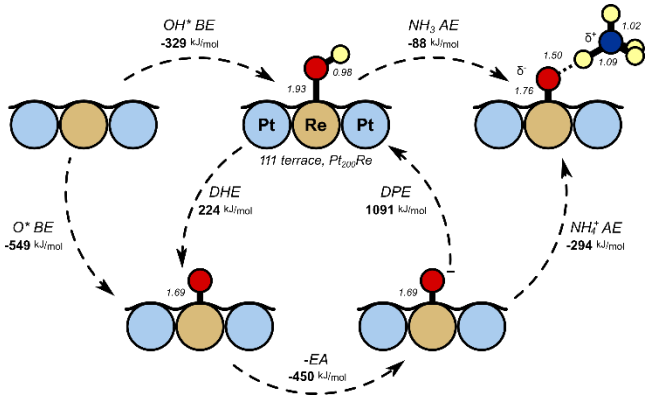

Figure S1. Born-Haber cycles for the deprotonation and NH_3 adsorption processes on a ReOx-modified Pt nanoparticle.

Table S1. Effect of convergence criteria on calculated properties of a ReO_x-promoted Pt 201-atom metal particle.

Convergence Properties:	*FFT Grid Size / Energy Cutoff (eV)*	*1.5*	*2.0*
	Wavefunction Convergence (eV)	*10^{-4}*	*10^{-6}*
	Energy Cutoff (eV)	*396*	*500*
Calculated Properties	*DPE (kJ mol^{-1})*	*1091*	*1085*
	DHE (kJ mol^{-1})	*224*	*220*
	eAff (kJ mol^{-1})	*450*	*448*

Table S2. Results for MO_x-promoted Pt clusters.

												MOH-NH_3 Bond Lengths		
Bulk	*Alloy*	*Site*	*CN*	*O BE* kJ mol^{-1}	*OH BE* kJ mol^{-1}	*NH_3 AE* kJ mol^{-1}	*DHE* kJ mol^{-1}	*EA* kJ mol^{-1}	*WF* kJ mol^{-1}	*DPE* kJ mol^{-1}	*DPE^{WF}* kJ mol^{-1}	*M-O* Å	*O-H* Å	*H-N* Å
Pt	**Pt**	*111 terrace*	9	-251	-210	-39	403	453	527	1267	1192	1.96	1.02	1.73
		100 terrace	8	-278	-215	-41	381	451	526	1247	1172	1.95	1.02	1.73
		edge11	7	-315	-251	-42	381	455	529	1243	1168	1.94	1.01	1.78
		edge10	7	-314	-244	-39	375	454	528	1238	1163	1.95	1.02	1.77
		corner6	6	-338	-258	-40	364	454	529	1227	1152	1.92	1.02	1.67
	Mo	*111 terrace*	9	-537	-326	-95	233	451	525	1099	1025	1.76	1.49	1.10
		100 terrace	8	-547	-362	-77	259	451	524	1125	1051	1.79	1.43	1.12
		edge11	7	-599	-403	-78	248	453	527	1111	1038	1.79	1.31	1.18
		edge10	7	-610	-419	-86	253	452	526	1118	1044	1.79	1.45	1.11
		corner6	6	-651	-450	-80	243	453	527	1107	1033	1.79	1.31	1.18
	Ru	*111 terrace*	9	-412	-266	-47	299	451	525	1164	1090	1.87	1.05	1.61
		100 terrace	8	-447	-295	-53	293	451	524	1159	1085	1.87	1.06	1.57
		edge11	7	-483	-320	-56	281	452	526	1145	1071	1.86	1.04	1.61
		edge10	7	-496	-328	-63	277	451	525	1142	1068	1.78	1.12	1.42
		corner6	6	-529	-345	-59	260	452	526	1124	1050	1.84	1.06	1.55
	W	*111 terrace*	9	-577	-360	-104	228	451	525	1093	1019	1.75	1.50	1.09
		100 terrace	8	-583	-384	-88	245	451	525	1111	1037	1.78	1.46	1.11
		edge11	7	-643	-436	-89	238	453	527	1101	1027	1.78	1.38	1.14
		edge10	7	-653	-450	-96	242	452	526	1107	1032	1.77	1.48	1.10
		corner6	6	-705	-497	-88	237	453	528	1100	1026	1.78	1.35	1.16
	Re	*111 terrace*	9	-549	-329	-88	224	450	524	1091	1017	1.76	1.50	1.09
		100 terrace	8	-560	-356	-87	240	451	524	1106	1033	1.78	1.52	1.09
		edge11	7	-630	-400	-95	215	452	526	1079	1005	1.77	1.44	1.11
		edge10	7	-642	-416	-107	219	451	525	1084	1010	1.76	1.50	1.09
		corner6	6	-702	-458	-102	201	452	526	1065	991	1.76	1.45	1.11

Table S3. Results for MO_x-promoted Rh clusters.

												MOH-NH_3 Bond Lengths		
Bulk	*Alloy*	*Site*	*CN*	*O BE* kJ mol^{-1}	*OH BE* kJ mol^{-1}	*NH_3 AE* kJ mol^{-1}	*DHE* kJ mol^{-1}	*EA* kJ mol^{-1}	*WF* kJ mol^{-1}	*DPE* kJ mol^{-1}	*DPE^{WF}* kJ mol^{-1}	*M-O* Å	*O-H* Å	*H-N* Å
Rh	**Rh**	*111 terrace*	9	-303	-233	-33	375	389	464	1302	1227	1.97	1.01	1.86
		100 terrace	8	-345	-249	-32	349	389	463	1276	1202	1.95	1.01	1.81
		edge11	7	-382	-276	-34	338	391	467	1263	1188	1.93	1.01	1.78
		edge10	7	-392	-283	-38	335	391	465	1260	1186	1.92	1.01	1.72
		corner6	6	-414	-297	-36	327	392	467	1251	1176	1.90	1.02	1.72
	Mo	*111 terrace*	9	-536	-325	-71	233	389	464	1161	1086	1.79	1.44	1.12
		100 terrace	8	-548	-356	-51	252	388	462	1180	1106	1.88	1.05	1.57
		edge11	7	-584	-391	-55	252	391	466	1178	1103	1.86	1.07	1.54
		edge10	7	-599	-409	-59	254	390	465	1181	1106	1.86	1.07	1.53
		corner6	6	-624	-442	-57	262	392	467	1187	1112	1.85	1.06	1.53
	Ru	*111 terrace*	9	-406	-259	-38	298	389	463	1226	1151	1.94	1.02	1.74
		100 terrace	8	-443	-293	-38	294	388	462	1223	1148	1.92	1.02	1.77
		edge11	7	-479	-316	-42	282	391	466	1208	1133	1.89	1.03	1.71
		edge10	7	-502	-330	-48	273	389	465	1200	1125	1.88	1.03	1.65
		corner6	6	-531	-355	-45	269	391	466	1194	1119	1.86	1.03	1.63
	W	*111 terrace*	9	-576	-356	-82	224	389	465	1152	1076	1.77	1.47	1.11
		100 terrace	8	-591	-382	-58	236	389	463	1164	1090	1.84	1.12	1.41
		edge11	7	-630	-422	-63	237	391	466	1163	1088	1.79	1.49	1.11
		edge10	7	-643	-439	-65	240	390	465	1166	1091	1.84	1.10	1.44
		corner6	6	-676	-479	-65	248	392	467	1173	1097	1.83	1.08	1.46
	Re	*111 terrace*	9	-542	-314	-71	216	388	463	1145	1070	1.85	1.13	1.40
		100 terrace	8	-556	-349	-48	238	388	462	1166	1092	1.88	1.05	1.61
		edge11	7	-611	-386	-69	219	390	465	1146	1071	1.78	1.54	1.09
		edge10	7	-630	-405	-69	220	389	464	1147	1072	1.83	1.12	1.42
		corner6	6	-676	-451	-70	220	391	466	1145	1070	1.81	1.11	1.40

Table S4. Results for MO_x-promoted Au clusters.

												MOH-NH₃ Bond Lengths		
Bulk	***Alloy***	***Site***	***CN***	***O BE*** *kJ mol^{-1}*	***OH BE*** *kJ mol^{-1}*	***NH₃ AE*** *kJ mol^{-1}*	***DHE*** *kJ mol^{-1}*	***EA*** *kJ mol^{-1}*	***WF*** *kJ mol^{-1}*	***DPE*** *kJ mol^{-1}*	***DPE^{WF}*** *kJ mol^{-1}*	***M-O*** *Å*	***O-H*** *Å*	***H-N*** *Å*
Au	**Au**	*111 terrace*	9	-153	-159	-22	450	412	483	1355	1284	2.09	1.00	1.87
		100 terrace	8	-195	-188	-28	437	409	477	1345	1277	2.05	1.00	1.91
		edge11	7	-187	-188	-24	445	410	482	1352	1280	2.05	1.00	1.89
		edge10	7	-188	-188	-33	445	410	482	1351	1279	2.06	0.99	1.91
		corner6	6	-200	-201	-24	445	412	484	1350	1278	2.02	1.00	1.83
	Mo	*111 terrace*	9	-590	-333	-94	187	406	477	1098	1027	1.75	1.47	1.10
		100 terrace	8	-626	-382	-79	201	407	477	1111	1041	1.77	1.43	1.12
		edge11	7	-676	-424	-83	192	407	478	1101	1030	1.77	1.36	1.15
		edge10	7	-679	-422	-85	188	408	478	1097	1026	1.76	1.43	1.12
		corner6	6	-732	-473	-86	186	407	478	1096	1025	1.77	1.40	1.13
	Ru	*111 terrace*	9	-385	-245	-38	305	408	478	1213	1143	1.91	1.02	1.74
		100 terrace	8	-461	-298	-44	281	408	477	1189	1120	1.87	1.02	1.70
		edge11	7	-482	-316	-42	279	407	478	1188	1117	1.86	1.03	1.67
		edge10	7	-489	-319	-46	275	407	478	1185	1113	1.86	1.02	1.76
		corner6	6	-529	-341	-47	257	407	478	1167	1096	1.84	1.05	1.59
	W	*111 terrace*	9	-651	-372	-117	165	406	477	1076	1005	1.74	1.53	1.09
		100 terrace	8	-683	-412	-101	173	407	477	1083	1013	1.75	1.47	1.11
		edge11	7	-740	-466	-102	170	407	478	1080	1008	1.75	1.42	1.12
		edge10	7	-715	-434	-105	164	407	479	1073	1002	1.74	1.48	1.11
		corner6	6	-784	-512	-97	173	407	478	1082	1011	1.75	1.43	1.12
	Re	*111 terrace*	9	-569	-309	-84	185	406	477	1096	1025	1.73	1.53	1.09
		100 terrace	8	-619	-372	-77	197	407	477	1107	1037	1.75	1.49	1.10
		edge11	7	-680	-407	-86	171	406	477	1082	1011	1.75	1.42	1.12
		edge10	7	-667	-401	-81	179	407	477	1089	1018	1.74	1.50	1.10
		corner6	6	-744	-461	-95	162	406	477	1072	1001	1.74	1.47	1.10

Table S5. Results for MO_x-promoted Ir clusters.

												MOH-NH₃ Bond Lengths		
Bulk	***Alloy***	***Site***	***CN***	***O BE*** *kJ mol^{-1}*	***OH BE*** *kJ mol^{-1}*	***NH₃ AE*** *kJ mol^{-1}*	***DHE*** *kJ mol^{-1}*	***EA*** *kJ mol^{-1}*	***WF*** *kJ mol^{-1}*	***DPE*** *kJ mol^{-1}*	***DPE^{WF}*** *kJ mol^{-1}*	***M-O*** *Å*	***O-H*** *Å*	***H-N*** *Å*
Ir	**Ir**	*111 terrace*	9	-313	-234	-39	366	431	505	1252	1178	1.97	1.01	1.77
		100 terrace	8	-360	-251	-40	336	430	503	1222	1149	1.95	1.02	1.75
		edge11	7	-430	-304	-49	319	432	506	1203	1129	1.92	1.01	1.82
		edge10	7	-439	-298	-48	303	431	505	1188	1114	1.91	1.04	1.65
		corner6	6	-492	-332	-53	285	432	506	1169	1095	1.88	1.04	1.60
	Mo	*111 terrace*	9	-524	-319	-89	239	431	505	1125	1051	1.77	1.42	1.12
		100 terrace	8	-543	-356	-67	257	430	503	1144	1071	1.80	1.43	1.13
		edge11	7	-577	-390	-65	258	432	506	1142	1068	1.84	1.09	1.46
		edge10	7	-594	-410	-72	260	431	506	1146	1072	1.80	1.45	1.12
		corner6	6	-621	-440	-66	264	433	507	1147	1073	1.83	1.10	1.43
	Ru	*111 terrace*	9	-374	-241	-41	312	430	504	1198	1124	1.94	1.02	1.73
		100 terrace	8	-404	-271	-43	311	430	503	1198	1124	1.91	1.03	1.69
		edge11	7	-461	-315	-49	299	432	506	1184	1110	1.88	1.02	1.69
		edge10	7	-478	-317	-49	284	431	505	1169	1095	1.81	1.37	1.16
		corner6	6	-519	-349	-55	274	432	506	1159	1085	1.84	1.06	1.52
	W	*111 terrace*	9	-570	-354	-102	229	431	506	1114	1040	1.75	1.49	1.10
		100 terrace	8	-595	-393	-79	243	430	503	1129	1056	1.78	1.46	1.11
		edge11	7	-628	-431	-72	247	432	507	1131	1057	1.82	1.13	1.38
		edge10	7	-645	-447	-83	247	432	506	1132	1057	1.78	1.49	1.11
		corner6	6	-683	-490	-74	252	433	507	1135	1061	1.81	1.13	1.37
	Re	*111 terrace*	9	-527	-300	-93	217	430	504	1103	1030	1.74	1.54	1.08
		100 terrace	8	-546	-348	-69	247	430	503	1134	1061	1.79	1.45	1.11
		edge11	7	-604	-394	-68	234	432	506	1119	1045	1.82	1.12	1.40
		edge10	7	-623	-406	-91	228	431	505	1113	1040	1.78	1.52	1.10
		corner6	6	-676	-454	-80	223	432	506	1107	1033	1.79	1.29	1.20

Table S6. Results for MO_x-promoted Ru clusters.

												MOH-NH₃ Bond Lengths		
Bulk	*Alloy*	*Site*	*CN*	*O BE* kJ mol^{-1}	*OH BE* kJ mol^{-1}	*NH₃ AE* kJ mol^{-1}	*DHE* kJ mol^{-1}	*EA* kJ mol^{-1}	*WF* kJ mol^{-1}	*DPE* kJ mol^{-1}	*DPE^{WF}* kJ mol^{-1}	*M-O* Å	*O-H* Å	*H-N* Å
Ru	**Ru**	*111 terrace*	9	-410	-262	-35	297	360	443	1253	1171	1.97	1.00	1.92
		100 terrace	8	-482	-313	-39	276	368	441	1225	1152	1.91	1.02	1.71
		edge11	7	-490	-322	-43	276	370	445	1223	1148	1.90	1.00	1.86
		edge10	7	-498	-335	-43	281	369	444	1228	1153	1.89	1.03	1.65
		corner6	6	-526	-356	-42	275	371	446	1220	1146	1.88	1.01	1.79
	Mo	*111 terrace*	9	-552	-348	-64	240	369	444	1188	1113	1.83	1.09	1.46
		100 terrace	8	-578	-391	-48	257	368	441	1205	1132	1.88	1.04	1.62
		edge11	7	-585	-397	-51	257	370	445	1203	1128	1.88	1.01	1.73
		edge10	7	-588	-400	-54	257	370	445	1203	1128	1.88	1.04	1.60
		corner6	6	-614	-433	-45	263	372	447	1208	1133	1.87	1.03	1.66
	W	*111 terrace*	9	-597	-378	-76	225	369	444	1173	1098	1.77	1.46	1.11
		100 terrace	8	-622	-414	-56	237	368	441	1186	1112	1.86	1.07	1.52
		edge11	7	-634	-430	-53	241	370	445	1187	1112	1.86	1.03	1.65
		edge10	7	-640	-433	-63	237	370	445	1184	1109	1.85	1.06	1.53
		corner6	6	-672	-473	-54	245	372	447	1190	1115	1.85	1.05	1.59
	Re	*111 terrace*	9	-552	-319	-73	211	369	443	1159	1085	1.76	1.49	1.10
		100 terrace	8	-587	-378	-50	235	368	441	1184	1111	1.87	1.05	1.59
		edge11	7	-610	-392	-54	226	370	444	1173	1098	1.87	1.01	1.73
		edge10	7	-614	-399	-58	230	369	444	1178	1103	1.86	1.05	1.55
		corner6	6	-662	-441	-54	224	371	446	1170	1095	1.84	1.06	1.57

Relationship between electron affinity and work function 201-metal-atom clusters

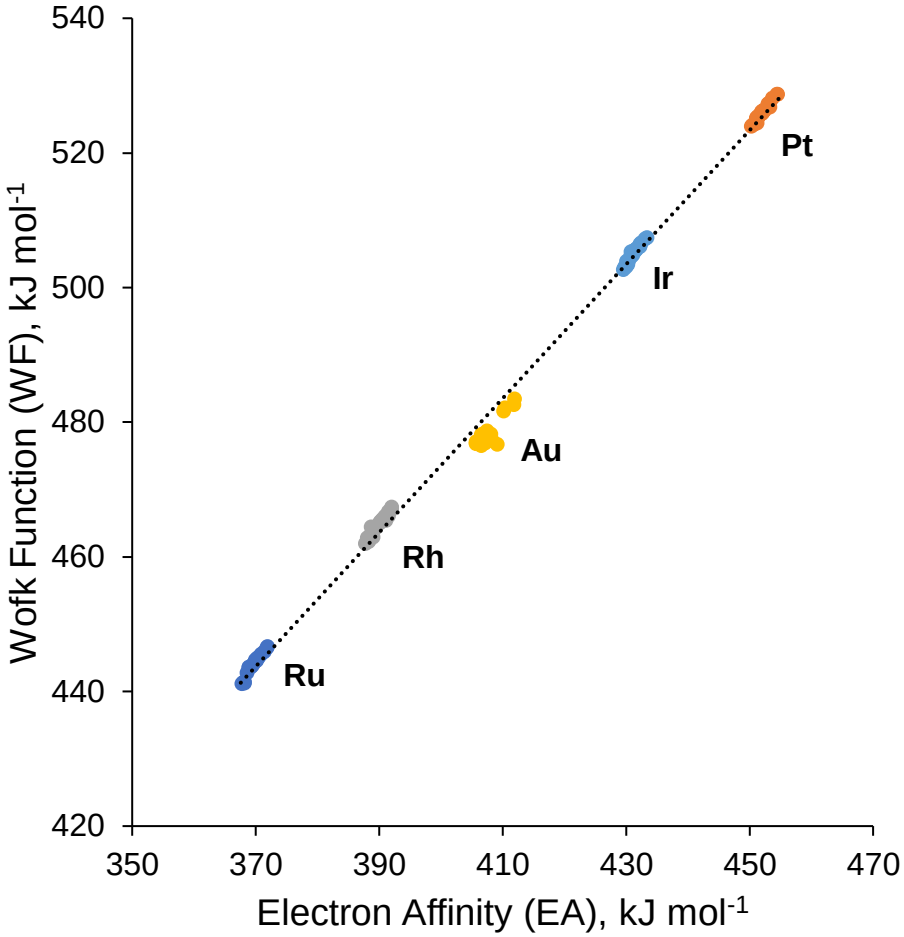

Figure S2. Relationship between the electron affinity (EA) and work function (WF) of MO_x-promoted M_{201} particles.

There is a linear relationship between electron affinity (EA) and work function (WF) as shown in Fig. S2 and, as observed, a single trend connects all studied alloy compositions, although alloys containing bulk Au fall slightly off the line compared to the others. This strong correlation indicates that calculating the DPE based on the EA or the WF will only shift the DPE values and not alter the observed trends in the manuscript or significantly reduce scatter in any of the relationships between DPE and other calculated characteristics.

The offset of ~75 kJ mol-1 relates to electron-electron repulsion caused by the increased charge on the 201-atom particle which is not captured during work function calculations. This charge concentrates on the surface of the particle, indicating that the difference between work function and electron affinity decreases with increasing particle size (which increases the surface area of the particle) as shown in Fig. S3 for both Rh and Pt particles from 13 to 586 atoms. Ionization energy (IE) is the energy to remove an electron from the particle (rather than add it) and it has a significantly higher value than the WF and also converges towards the WF with

increasing particle size (Fig. S3). The average of the IE and the EA is very close to the calculated WF.

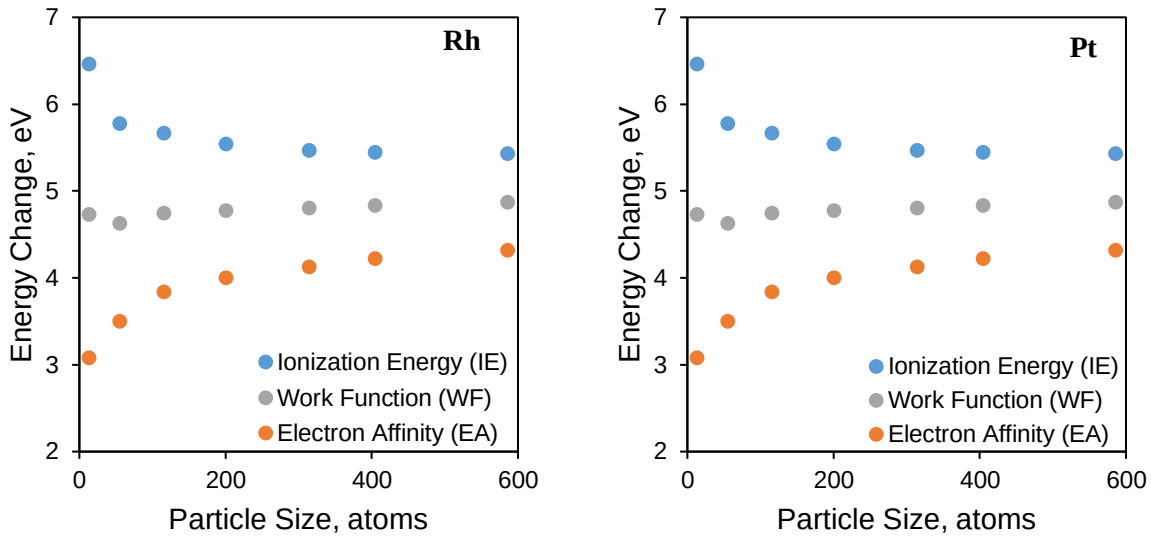

Figure S3. Ionization energy (IE), work function (WF) and electron affinity (EA) as a function of particle size for 13- to 586-atom Rh and Pt particles.

Effects of MOH site on Acid Strength

As you decrease the coordination number of the metal atom to which the oxygen binds, bond-order-conservation would predict an increase in the BE strength (more negative value). Fig. S4 contains box and whisker plots for the BE of oxygen to metal atoms with different coordination numbers for all of the metal clusters examined in this work. As the CN decreases from 9 for (111) terraces sites to 6 for corner sites, the average O* BE becomes stronger, decreasing from -480 kJ mol^{-1} to -600 kJ mol^{-1}. A closer analysis of the differences in O* BE between the coordinatively less-saturated sites and the (111) terrace site reported in Fig. S4 show that the increase in binding strength between edge (CN=7) and (111) terrace (CN=9) sites ranges from 33 to 127 kJ mol^{-1}, with an average of 74 kJ mol^{-1} across the systems studied. Corner (CN=6) sites show even greater increase in the M–O binding strength with an average increase of 118 kJ mol^{-1} over that on the (111) terrace sites.

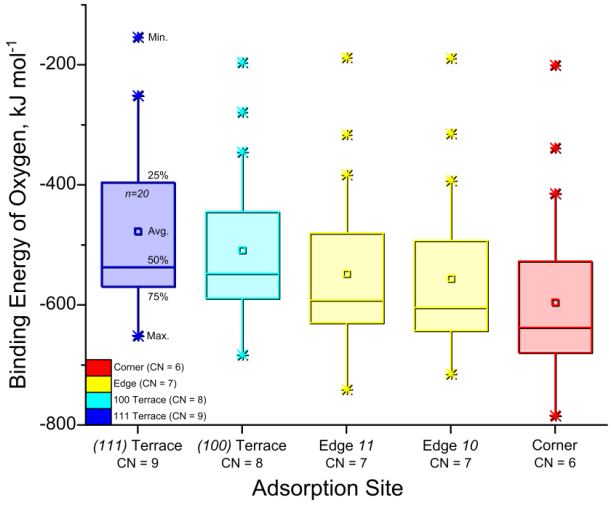

Figure S4. Box and whisker plots for the binding energies of oxygen to different sites on the 201-atom metal nanoparticles. The box outlines the 25th and 75th percentiles with the line in the box representing the median value and the square (□) representing the average and the "whiskers" are extended to the 90th percentiles. As the coordination number of the binding site decreases, the BE becomes stronger.

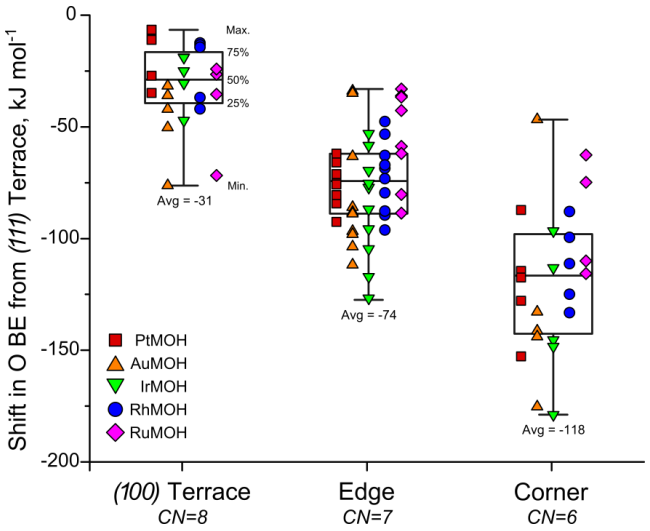

Figure S5. The difference in the BE of oxygen between the highly coordinated (111) terrace site (CN = 9) and lower coordinated sites (CNs 6-8). The box outlines the 25th and 75th percentiles with the line in the box representing the median value and the square (□) representing the average and the "whiskers" are extended to the 90th percentiles.

The calculated binding energies for OH* intermediates increased in a very similar manner as those for the binding energies for O* thus indicating that the changes in DHE at different metal surface sites is small. The changes in DHE between the less-coordinatively saturated sites and the (111) terrace site for each of the alloys studied are plotted in Fig. S6. The results for the binding of OH* on pure metal nanoparticles indicate that decreasing the CN of the metal atom to which the OH* is bound weakens the O-H bond, as expected, although the magnitude of the shift has a fairly wide range (-5 to -82 for OH* bound to the corner site of the five pure metals). For Ru-promoted alloys, the changes in DHE with changes in metal atom coordination are somewhat smaller, with average decreases in the O-H bond strength of 8, 22 and 38 kJ mol^{-1} for the (100) terrace, edge and corner sites, respectively; the weakening of the O-H bond that results from decreasing the coordination number of the metal to which it is bound is again consistent with bond-order-conservation principles. The shifts in DHE over metal clusters with ReOx promoters, however, were not always negative, in some cases, the OH* that is bound to the coordinatively less saturated metal atom actually resulted in stronger O-H bond energies (and stronger O–M bond energies) than those bound to a metal atom in (111) terrace. For WO_x and MoO_x promoters, the O–H bond is consistently stronger at lower-coordinated metal sites than at the (111) terrace site. It is unclear why this is true, as it is inconsistent with bond-order-conservation principles. Although, it does seem that there is a periodic effect with a Ru site (group 8) showing a weakening in the O–H bond with increasing M–O bond strength, a Re site

(group 7) showing a mixture of weakening and strengthening of the O–H bond and Mo and W sites (both group 6) showing a strengthening of the O–H bond with increasing M-O bond strength. Overall, there does not appear to be a consistent trend between the coordination number of the metal atom and the O–H bond strength of the adsorbed OH*. As stated previously, the acidity (as measured by DPE) of a site is directly proportional to the O–H bond strength (as measured by DHE) so, as shown in Tables S1-S5, there are 11 alloys in which the most acidic site is the corner and 11 alloys in which the most acidic site is the (111) terrace.

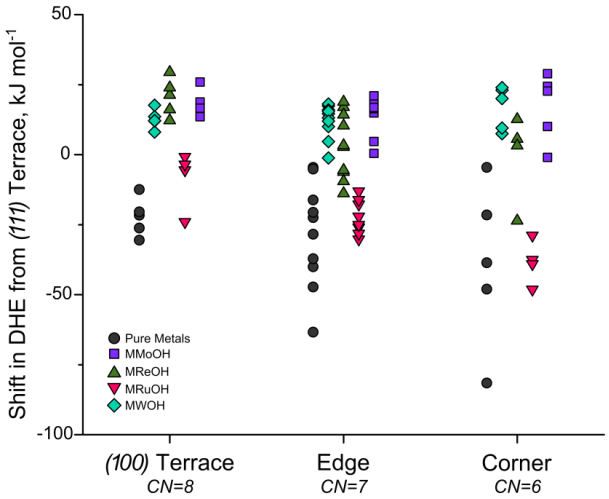

Figure S6. The difference in DHE between the highly coordinated (111) terrace site (CN = 9) and lower coordination sites (CNs 6-8). Pure metal nanoparticles and Ru-promoted nanoparticles show an overall decrease in the O-H bond strength as the CN decreases. However, Re, Ru and W-promoted nanoparticles show an overall increase in O-H bond strength with decreasing CN.

Geometry and protonation of NH_3 on MOH sites

A close analysis of the geometric structures of the MO–H–NH_3 complexes that form upon the adsorption of NH_3 adsorption to the different M–OH acid sites revealed a relationship between the O—H and H—N bond distances as observed. Fig. S7 displays this correlation, which is similar to previously reported work on HPAs [33]. According to bond order conservation, it is expected that as the N–H bond order increases, the O–H bond order must decrease. [34] Bond order conservation can be used to directly relate the changes in bond order to bond length according to Eq. 7, in which r_0 represents the equilibrium distance of the two–body system. Rearrangement of Eq. 7 produces Eq. 8, which was used to generate the fit between the distance between the proton and the N on the ammonia (H-Adsorbate) and the proton and the O of the zeolite (MO-H) distances shown in Fig. S7.

$$X = x_{OH} + x_{NH} = 1 \quad (6)$$

$$x(r) = \exp\{-(r - r_0)/b\} \quad (7)$$

$$r_{OH} = -b_{OH}*\ln[1-\exp(-(r_{NH} - r_{0,NH})/b_{NH})] + r_{0,OH} \quad (8)$$

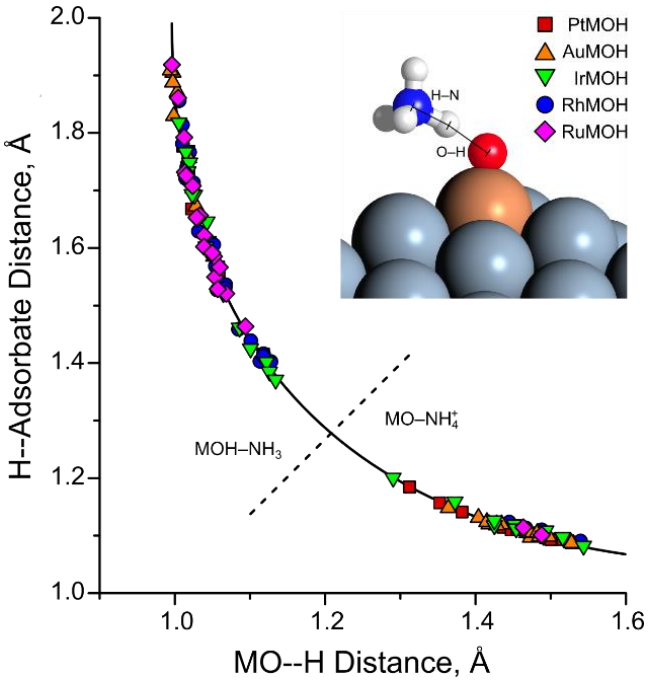

Figure S7. Proton–ammonia (H^+–N) and proton–oxygen (H^+–O) bond lengths of ammonia bound to a variety of MOH surface alloys.

Fig. S7 also shows a distinct gap in O–H bond lengths between ~1.15 and 1.3 Å which demonstrates that at a certain acidity, the proton will shift from being bound to the MO site to the nitrogen on the ammonia to form the ammonium ion (NH_4^+) which is bound further away from the negatively charged MO(-) site through coulombic interactions in the NH_4^+–$^-$OM ion pair. Unlike previous studies over HPAs, in which this always occurred for NH_3 adsorption, the wide range of acidity of the MOH systems studied here reveal a range of DPE values where the interaction with the basic N on NH_3 may or may not result in the deprotonation of the acid site. Fig. S8 shows the O—H and N—H bond distances against the DPE. The results show that the transition from adsorbed ammonia to the ammonium complex occurs over a range of DPE values, from 1130 and 1180 kJ mol^{-1} where both ammonia and ammonium are observed. DPE values lower than 1130 result in only ammonium whereas DPE values above 1180 result only in ammonia adsorption.

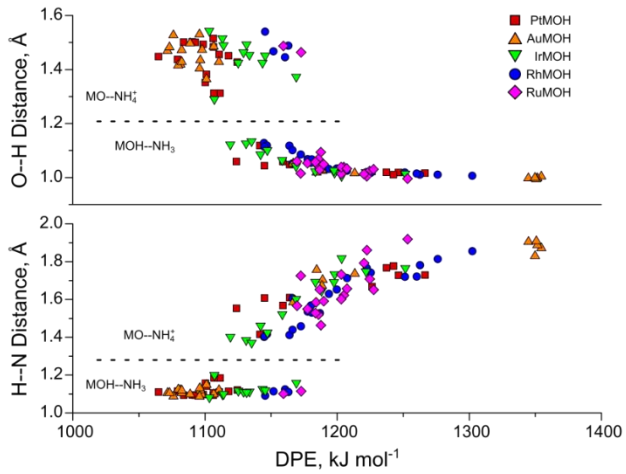

Figure S8. The correlation between the O--H and N--H distances for adsorbed ammonia verses the deprotonation energy. N–H bond lengths ≤ 1.3 or O–H bond lengths > 1.2 indicate ammonium ions have been formed. At DPE > 1180, ammonia only chemisorbs or physisorbs to the MOH cluster. When the DPE is lower than 1130, the MOH clusters deprotonate, forming strongly bound ammonium cations. Between DPE of 1180 and 1130, both ammonia and ammonium species are observed, depending on the alloy and MOH site.

Transition State Structure

```
TITL CONTCAR
CELL 0.0000 10.7605 10.7605 21.5894 90.0000 90.0000 120.0000
LATT -1
SFAC Rh Re O H C
Rh    1    0.00000    0.00000    0.00463    1.00000    0.00000
Rh    1    0.99799    0.49909    0.31112    1.00000    0.00000
Rh    1    0.83333    0.16667    0.10637    1.00000    0.00000
Rh    1    0.83333    0.66667    0.10637    1.00000    0.00000
Rh    1    0.66781    0.33043    0.21206    1.00000    0.00000
Rh    1    0.49917    0.99871    0.30988    1.00000    0.00000
Rh    1    0.66630    0.83361    0.20776    1.00000    0.00000
Rh    1    0.49997    0.50095    0.30988    1.00000    0.00000
Rh    1    0.00000    0.25000    0.00463    1.00000    0.00000
Rh    1    0.00000    0.75000    0.00463    1.00000    0.00000
Rh    1    0.50000    0.25000    0.00463    1.00000    0.00000
Rh    1    0.00000    0.50000    0.00463    1.00000    0.00000
Rh    1    0.50000    0.75000    0.00463    1.00000    0.00000
Rh    1    0.33333    0.41667    0.10637    1.00000    0.00000
Rh    1    0.16709    0.08448    0.20777    1.00000    0.00000
Rh    1    0.33333    0.91667    0.10637    1.00000    0.00000
Rh    1    0.16609    0.58229    0.20751    1.00000    0.00000
Rh    1    0.99788    0.24847    0.31087    1.00000    0.00000
Rh    1    0.99990    0.74974    0.31109    1.00000    0.00000
Rh    1    0.83333    0.41667    0.10637    1.00000    0.00000
Rh    1    0.66909    0.08744    0.21021    1.00000    0.00000
Rh    1    0.83333    0.91667    0.10637    1.00000    0.00000
Rh    1    0.50000    0.00000    0.00463    1.00000    0.00000
Rh    1    0.66632    0.58196    0.20733    1.00000    0.00000
Rh    1    0.49836    0.24802    0.31587    1.00000    0.00000
Rh    1    0.49998    0.74997    0.31126    1.00000    0.00000
Rh    1    0.25000    0.25000    0.00463    1.00000    0.00000
Rh    1    0.25000    0.75000    0.00463    1.00000    0.00000
Rh    1    0.08333    0.41667    0.10637    1.00000    0.00000
Rh    1    0.08333    0.91667    0.10637    1.00000    0.00000
Rh    1    0.75000    0.25000    0.00463    1.00000    0.00000
Rh    1    0.75000    0.75000    0.00463    1.00000    0.00000
Rh    1    0.58333    0.41667    0.10637    1.00000    0.00000
Rh    1    0.50000    0.50000    0.00463    1.00000    0.00000
Rh    1    0.41667    0.08327    0.20810    1.00000    0.00000
Rh    1    0.58333    0.91667    0.10637    1.00000    0.00000
Rh    1    0.41654    0.58324    0.20787    1.00000    0.00000
Rh    1    0.24872    0.25032    0.31087    1.00000    0.00000
Rh    1    0.24978    0.74893    0.31174    1.00000    0.00000
Rh    1    0.91665    0.08317    0.20743    1.00000    0.00000
Rh    1    0.91661    0.58330    0.20738    1.00000    0.00000
Rh    1    0.74961    0.74967    0.31236    1.00000    0.00000
Rh    1    0.25000    0.00000    0.00463    1.00000    0.00000
Rh    1    0.33333    0.16667    0.10637    1.00000    0.00000
```

```
Rh    1    0.25000    0.50000    0.00463    1.00000    0.00000
Rh    1    0.08333    0.16667    0.10637    1.00000    0.00000
Rh    1    0.08333    0.66667    0.10637    1.00000    0.00000
Rh    1    0.75000    0.00000    0.00463    1.00000    0.00000
Rh    1    0.75000    0.50000    0.00463    1.00000    0.00000
Rh    1    0.58333    0.16667    0.10637    1.00000    0.00000
Rh    1    0.58333    0.66667    0.10637    1.00000    0.00000
Rh    1    0.41813    0.33313    0.20868    1.00000    0.00000
Rh    1    0.24800    0.99823    0.30960    1.00000    0.00000
Rh    1    0.41758    0.83356    0.20743    1.00000    0.00000
Rh    1    0.33333    0.66667    0.10637    1.00000    0.00000
Rh    1    0.24903    0.49967    0.31062    1.00000    0.00000
Rh    1    0.91433    0.33240    0.20928    1.00000    0.00000
Rh    1    0.75093    0.00012    0.31122    1.00000    0.00000
Rh    1    0.91542    0.83247    0.20810    1.00000    0.00000
Rh    1    0.75166    0.50120    0.31048    1.00000    0.00000
Rh    1    0.16656    0.33385    0.20715    1.00000    0.00000
Rh    1    0.99969    0.99959    0.31076    1.00000    0.00000
Rh    1    0.16716    0.83238    0.20785    1.00000    0.00000
Re    2    0.75321    0.24973    0.32283    1.00000    0.00000
 O    3    0.73887    0.24507    0.40450    1.00000    0.00000
 O    3    0.50200    0.24280    0.42037    1.00000    0.00000
 O    3    0.75675    0.50484    0.54204    1.00000    0.00000
 O    3    0.04203    0.66959    0.53165    1.00000    0.00000
 O    3    0.66894    0.78076    0.49230    1.00000    0.00000
 H    4    0.59275    0.23628    0.42427    1.00000    0.00000
 H    4    0.38531    0.04381    0.46417    1.00000    0.00000
 H    4    0.29004    0.13329    0.44342    1.00000    0.00000
 H    4    0.52004    0.22612    0.54523    1.00000    0.00000
 H    4    0.33456    0.15920    0.55784    1.00000    0.00000
 H    4    0.48016    0.42661    0.56525    1.00000    0.00000
 H    4    0.34799    0.37089    0.50583    1.00000    0.00000
 H    4    0.53740    0.48562    0.42845    1.00000    0.00000
 H    4    0.78401    0.57414    0.44884    1.00000    0.00000
 H    4    0.67117    0.62386    0.49193    1.00000    0.00000
 H    4    0.86390    0.56243    0.54205    1.00000    0.00000
 H    4    0.07621    0.66893    0.48981    1.00000    0.00000
 H    4    0.10506    0.65549    0.55952    1.00000    0.00000
 H    4    0.67123    0.80771    0.44854    1.00000    0.00000
 H    4    0.74991    0.86298    0.51183    1.00000    0.00000
 C    5    0.42351    0.22096    0.52565    1.00000    0.00000
 C    5    0.44769    0.37485    0.51977    1.00000    0.00000
 C    5    0.56270    0.45921    0.47404    1.00000    0.00000
 C    5    0.39079    0.14841    0.46286    1.00000    0.00000
 C    5    0.70850    0.52935    0.48780    1.00000    0.00000
END
```